J Vet Intern Med 2013;27:1165–1171

Applicability of 3T Body MRI in Assessment of Nonfocal Bone Marrow Involvement of Hematopoietic Neoplasia in Dogs

D.A. Feeney, L.C. Sharkey, S.M. Steward, K.L. Bahr, M.S. Henson, D. Ito, T.D. O'Brien, C.R. Jessen, B.D. Husbands, A. Borgatti, and J. Modiano

Background: The utility of whole body magnetic resonance imaging (MRI) in detecting bone marrow infiltration in dogs with cancer has not been investigated.

Objectives: To assess the feasibility of 3T body MRI for bone marrow assessment in dogs with hematopoietic neoplasia.

Animals: Seven dogs with B-cell lymphoma, 3 dogs with myelodysplastic syndrome (MDS), and 2 clinically normal dogs.

Methods: A prospective study of dogs with hematopoietic cancer was conducted using T1W, T2W, In-Phase, Out-of-Phase and STIR pulse sequences of the body excluding the head prior to bone marrow sampling. The relative signal intensity of a midlumbar vertebral body and a midshaft femoral bone marrow was compared by visual and point region of interest analysis to regional skeletal muscle.

Results: Similarity of femoral diaphyseal and vertebral body marrow signal intensity to that of skeletal muscle on the Out-of-Phase sequence was useful in distinguishing the 3 dogs with hypercellular marrow because of MDS from the 7 dogs with B-cell lymphoma and from the 2 clinically normal dogs. 1/7 dogs with lymphoma had proven bone marrow involvement but normal cellularity and less than 5% abnormal cells. Unaffected midfemoral marrow had greater signal intensity than skeletal muscle and unaffected vertebral marrow had less signal intensity than skeletal muscle on the Out-of-Phase sequence.

Conclusions and Clinical Importance: 3T, Out-of-Phase MR pulse sequence was useful in distinguishing diffuse bone marrow infiltrate (MDS) from minimally or unaffected marrow using skeletal muscle for signal intensity comparison on whole body MRI.

Key words: Lymphoma; Magnetic resonance; Marrow signal intensity; MR pulse sequence; Myelodysplasia.

Whole body magnetic resonance imaging (MRI) staging techniques in people and companion animals might provide prognostically relevant information in a cost-effective, minimally invasive manner.[1–5] Bone marrow involvement has particular prognostic relevance in dogs with hematopoetic malignancies.[6] There is information on imaging of normal marrow in dogs using low-field MRI techniques,[7,8] but nothing on high field, particularly 3T, and nothing with a spectrum of pulse sequences available. There is, however, a need to assess the potential applicability of high-field body MRI as a relevant bone marrow staging procedure in dogs with infiltrative (nonfocal) malignancies. Using 1.5T and 3.0T MRI techniques, characterization of marrow infiltrates in vertebral or long-bone diaphyseal yellow marrow in adult humans aids both staging and treatment efficacy.[9–14] There are potential inaccuracies of standard site marrow sampling in human beings,[15] but the applicability of MRI-based guidance for marrow staging in dogs has not been explored. Before any in-depth clinical investigation regarding the relevance of bone marrow imaging in dogs with hepatopoetic neoplasia using high-field MRI can be performed, it must be demonstrated that generally available high-field MRI techniques can define infiltrative malignant disease in the bone marrow of adult dogs during practical whole body imaging. If, based on preliminary results, infiltrative marrow malignancy can be identified, it would provide the impetus to further investigate body MRI as a means of staging these malignancies with regard to high-grade marrow disease as well as using it as a guide to sample marrow for confirmation and further staging of the disease.

Abbreviations:

3T	3 Tesla magnetic field strength
MDS	myelodysplastic syndrome
MRI	magnetic resonance imaging
ROI	region of interest
T1W	T1-weighted image (short TR, short TE)
T2W	T2-weighted image (long TR, Long TE)

Infiltrative (nonfocal) disease is an interpretive dilemma because the infiltrate cannot be measured and may be inflammatory, metabolic, pharmacologic, or neoplastic origin.[9,16–18] The identification of abnormalities is then based on the variances in tissue or organ "brightness" in the image as compared to some internal standard. Magnetic resonance imaging can detect paramagnetic substances (gadolinium-based contrast agents, iron-based contrast agents, and extravascular blood

From the Department of Veterinary Clinical Sciences (Feeney, Jessen); the Masonic Cancer Center (Sharkey, Henson, Ito, Borgatti, Modiano); and the Veterinary Medical Center (Steward), University of Minnesota, St. Paul, MN; the Metropolitan Veterinary Hospital, Akron, OH (Bahr); the Department of Veterinary Population Medicine, University of Minnesota, St. Paul, MN (O'Brien); and the Blue Pearl Veterinary Partners, Eden Prairie, MN (Husbands).

Corresponding author: Daniel A. Feeney, Department of Veterinary Clinical Sciences, University of Minnesota, 1365 Gortner Avenue, St. Paul, MN 55108; e-mail: feene001@umn.edu.

Submitted February 28, 2013; Revised April 22, 2013; Accepted June 6, 2013.

10.1111/jvim.12151

products), melanin, and proteinaceous substances in tissues,[19–22] and can emphasize tissue contrast using a versatile spectrum of MRI pulse sequences,[23–25] provided the normal appearance by pulse sequence is understood.[19,26–33] High-field muscle signal intensity has been used in people as an internal standard for bone marrow comparison,[34–37] but only low-field information on normal dogs could be found.[7,8]

The purpose of this prospective pilot study was to determine if data on a limited number of dogs with multicentric malignancies like lymphoma or myelodysplastic syndrome (MDS) compared to a limited number of clinically normal adult dogs provided sufficient justification to further explore body MRI for bone marrow staging.

Materials and Methods

Based on inclusion criteria of clinical and either cytologic or hematologic evidence of hematopoietic neoplasia (lymphoma or MDS), 10 dogs presenting to the U-MN Veterinary Medical Center Oncology Service for staging and treatment were subjected to body MR imaging and bone marrow sampling. A preliminary cytologic diagnosis of lymphoma in a lymph node was based on >50% medium to large or cytologically atypical lymphocytes. This was followed with histopathologic confirmation by examination of hematoxylin and eosin stained lymph node biopsy specimen and classification according to the World Health Organization criteria adapted for the dog.[38] A diagnosis of MDS was made based on data from the complete blood count and bone marrow evaluation (see below). Dogs were excluded from consideration for the study if there were unjustifiable risks associated with general anesthesia for the imaging procedure. All protocols were approved by the Institutional Animal Care and Use Committee and owner consent was obtained before the procedure.

Bone marrow sampling was performed at 2 sites per dog (iliac crest and proximal humerus) unless directed otherwise by unexplainable or asymmetric findings on the MRI images. The bone marrow sampling was performed immediately after the MRI. Using standard techniques, bone marrow aspirates and core biopsies were collected from each site using Rosenthal bone marrow aspirate needles and Jamshidi core biopsy needles, respectively. The bone marrow involvement in dogs with lymphoma was diagnosed by the presence of >2% lymphoblasts with a concurrent cytologic or histologic diagnosis of lymphoma in peripheral lymph nodes or accessible organs. The diagnosis of MDS was based on a modification of the most recent World Health Organization scheme for myeloid neoplasms.[39] that excludes the use of cytogenetic abnormalities based on the fact that these have not been characterized in dogs.[40] Briefly, the presence of refractory peripheral cytopenias in combination with evidence of dysplasia in >10% of precursors in one or more myeloid lineages (erythroid, myeloid, or megakaryocytic) and a blast count of <20% resulted in a diagnosis of MDS. The classifications of marrow pathology were compared to the MRI findings in an attempt to define trends that would justify acquiring data in a subsequent study suitable for statistical analysis. In the context of the pathologic diagnoses, marrow images were evaluated for the presence or absence of abnormal signal intensity or perturbations of the marrow architecture.

The body was divided into cranial (excluding the head) and caudal halves and the dogs were imaged using 3 Tesla MRI imaging equipment[a] under general anesthesia without respiratory or cardiac gaiting. At least two of the 3 standard (dorsal, sagittal, transverse) imaging planes were used for each pulse sequence to permit orthogonal comparison. The pulse sequences used included T1W fast spin echo (FSE) [TR = 825 ms, TE = 20 ms, 1 NEX], T2W FSE [TR = 3200 ms, TE = 120 ms, 1 NEX], in-phase [TR = 140 ms, TE = 2.1 ms, flip angle = 80°, 1 NEX], out-of-phase [TR = 140 ms, TE = 3.15 ms, flip angle = 80°, 1 NEX], and short tau inversion recovery (STIR) [TR = 3800 ms, TE = 34 ms, TI = 160 ms, 1 NEX]. Slice thickness was 8–10 mm with an interslice interval of 3–5 mm. The field of view was adjusted to body region imaged, but ranged from 30 to 45 cm. All sequences were completed in less than 75 minutes. As a baseline, 2 clinically normal young adult dogs in the elective small animal surgery spay/neuter program were subjected to the same imaging protocol.

All image interpretation was performed by the lead author (D.A.F.) without knowledge of bone marrow, lymph node, or parenchymal organ status other than that the dogs had suspected hematopoietic malignancy or were clinically normal. The signal intensity of lumbar vertebral marrow and middiaphyseal femoral marrow (slice chosen to limit partial volume effects) regions were visibly defined as low (similar to urinary bladder on T1W, In-phase, Out-of-phase; similar to skeletal muscle on T2W; similar to fat on STIR sequences), high (similar to fat on T1W, T2W FSE, In-phase, Out-of-phase; similar to urinary bladder on STIR sequences) or midrange (visually different from and between the extremes listed above). Further visual marrow signal intensity comparison was made specifically to regional skeletal muscle (classified as similar to, greater than or less than). In addition, representative, user-defined point ROI measurements from images on a picture archive and communication system[b] on the same tissue groups were made. Specifically, a left and a right hemivertebral body marrow signal intensity measurement were made on one of the midlumbar vertebrae from an axial image (specific vertebra chosen to limit partial volume artifact). Left and right muscle signal intensity measurements were made from the epaxial muscles in the same region as the vertebra being compared and all were from the same slice. Left and right measurements were averaged for both muscle and vertebral marrow before the marrow/muscle numeric signal intensity calculations (average marrow signal intensity divided by average muscle signal intensity) were made. Two marrow signal intensity measurements were made midfemur (diaphysis) with the choice of left versus right made based on the best image available from among the dorsal, axial, and sagittal planes and to limit partial volume artifact. Two regional skeletal muscle signal intensity measurements were also made in the muscles surrounding the middiaphyseal region sampled for marrow signal intensity and all were from the same slice. The 2 measurements were averaged for both muscle and midfemoral marrow before the marrow/muscle numeric signal intensity comparisons were made as described above for the lumbar vertebrae. A visual overview of both the upper torso and the lower torso was made to assure that the trends observed in the hind limbs were the same in the front limbs. Because this study was carried out to investigate both parenchymal organ signal intensity and bone marrow signal intensity in practical body imaging, specific positioning to optimize a specific long bone or a particular spinal segment was not performed. The images from the 2 clinically normal dogs were interpreted similarly, but individually such that the findings in one did not influence the findings in the other.

Because the study was intended as a proof of principle regarding whether lesions could be located by high-field MR body screening images and how what was found compared with the available information on the dog's bone marrow status, no statistical analyses were performed.

Results

The 2 healthy dogs were mixed-breed, intact males between the ages of 1.5 and 3 years old. The 10 clinically affected dogs in the study had an average age of 7.9 years (range 4.5–11). There were 5 neutered males (Akita, American Staffordshire Terrier, Scottish Terrier, Shetland Sheepdog, Standard Poodle) and 5 spayed females (Golden Retriever [3], mixed-breed, Shih Tzu). Seven dogs were diagnosed with high-grade B-cell lymphoma (4 stage 3a, 1 stage 4a, 2 stage 5a) and three with MDS. The % blast cells for six of the seven lymphoma-affected, but marrow negative dogs was less than 2% and marrow cellularity was either within or less than reference intervals. The lymphoma-affected, but marrow positive dog had 3.5% blast cells but cellularity still within reference intervals. By comparison, the MDS-affected dogs had 7–11% blast cells and cellularity above reference intervals. With the exception of Case 10, none of the dogs had prior steroid or cytotoxic treatment. Case 10 received systemic corticosteroid treatment for 84 days without satisfactory improvement before the MRI and bone marrow sampling.

Focal or multifocal bone marrow infiltrates were not found in either the canine diffuse B-cell lymphoma dogs or the MDS dogs. There was no protocol that distinguished the single marrow positive B-cell lymphoma-affected dog from the other 6 lymphoma-affected dogs without confirmed marrow involvement or from the clinically normal dogs. However, when the signal intensity relationship between the midfemoral and lumbar vertebral marrow regions and their regional skeletal muscle in each dog with hematopoietic neoplasia was compared to similar regions from the normal dogs, a number of variations were found across the various MR pulse sequences (Table 1; Fig 1 and 2). While only lumbar vertebral marrow and midfemoral marrow signal intensity were specifically analyzed here, the findings were visually similar in the front limb long bones. From among the 5 pulse sequences, only the Out-of-Phase protocol visually distinguished the abnormal lumbar vertebral and midfemoral marrow relative signal intensity in the MDS-affected dogs (both similar to skeletal muscle on that sequence) from both the vertebral and midfemoral marrow relative signal intensity in the normal and lymphoma-affected dogs (both visibly different from skeletal muscle on that sequence). As measured by point ROI and expressed in terms of numeric relative signal intensity using epaxial muscle signal intensity as a basis for comparison, the MDS-affected dogs had vertebral marrow signal intensities visibly similar to and numerically within 30% of that in skeletal muscle (ratio range from 0.70 to 1.02). The 2 normal and 7 lymphoma-affected dogs had notably less visible and lower numeric vertebral marrow signal intensity compared to muscle (vertebral body marrow/muscle ratio range 0.15–0.58). All MDS dogs had visually similar midfemoral marrow and muscle signal intensities whereas the 2 normal and the 7 lymphoma-affected

Table 1. Visible relative signal intensity @ 3T for skeletal muscle, urinary bladder (fluid), fat, lumbar vertebral marrow, and femoral marrow regions by MR pulse sequence from 7 dogs with lymphoma (L), 3 dogs with myelodysplastic syndrome (M), and 2 clinically normal (N) young adult dogs.

Relative Signal Intensity	T1W	T2W	In-Phase	Out-of-Phase	STIR
Low	Urinary bladder	Skeletal muscle	Urinary bladder	Urinary bladder	Fat
				Vertebral marrow (L)	
				Vertebral marrow (N)	
Mid	Skeletal muscle	Long bone marrow (M)	Long bone marrow (M)	Long bone marrow (M)	Long bone marrow (N)
	Vertebral marrow (L)	Vertebral marrow (L)	Skeletal muscle	Skeletal muscle	Long bone marrow (L)
		Vertebral marrow (M)	Vertebral marrow (L)	Vertebral marrow (M)	Long bone marrow (M)
		Vertebral marrow (N)	Vertebral marrow (N)		Skeletal muscle
			Vertebral marrow (M)		Vertebral marrow (L)
					Vertebral marrow (M)
					Vertebral marrow (N)
High	Fat	Fat	Fat	Fat	Urinary bladder
	Long bone marrow (M)	Long bone marrow (L)	Long bone marrow (N)	Long bone marrow (N)	
	Long bone marrow (N)	Long bone marrow(N)	Long bone marrow (L)	Long bone marrow (L)	
	Long bone marrow (L)	Urinary bladder			
	Vertebral marrow (N)				
	Vertebral marrow.(M)				

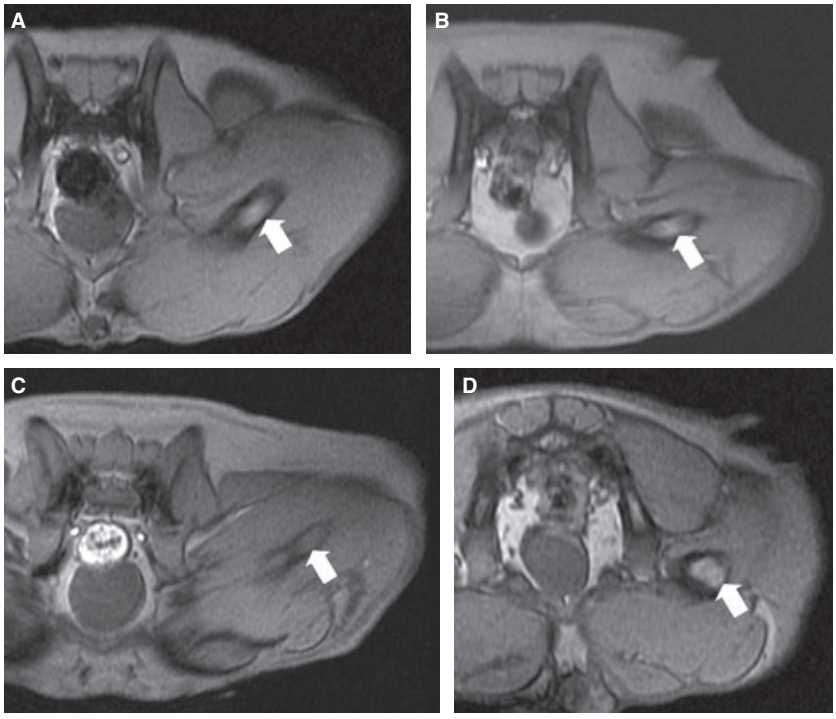

Fig 1. Comparison of axial out-of-phase middiaphyseal femoral images from a dog with hypocellular marrow and lymphoma (**A**), a dog with normocellular marrow and lymphoma (**B**), a dog with hypercellular marrow from myelodysplastic syndrome (**C**) and a clinically normal dog (**D**). Note the low signal intensity (similar to regional muscle) of the midfemoral diaphysis marrow (arrow) on the dog with hypercellular marrow because of myelodysplasia (C) in comparison with comparable regions in the other dogs (arrows).

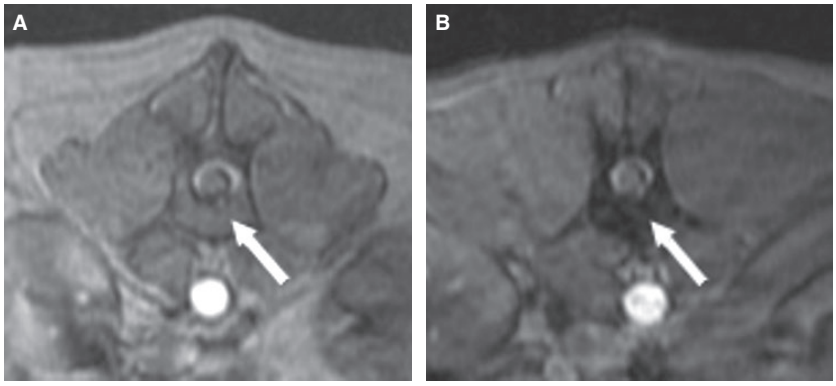

Fig 2. Comparison of axial out-of-phase lumbar vertebral images from a dog hypercellular marrow and myelodysplastic syndrome (**A**) and a clinically normal dog (**B**). Note the nearly identical signal intensity of vertebral body marrow (arrows) and the regional skeletal muscle in the dog with hypercellular marrow because of myelodysplasia (A) compared to the greatly different signal intensity of these tissues (vertebral marrow less than muscle) in a clinically normal dog (B).

dogs had marrow signal intensity notably greater than regional skeletal muscle at subjective visual examination. Two of the 3 MDS-affected dogs had midfemoral point ROI-based marrow signal intensity measurements that differed numerically by less than 3% from regional skeletal muscle (midfemoral marrow/muscle ratio range from 0.97 to 1.0). The 2 normal and 4/7 lymphoma-affected dogs had notably greater numeric midfemoral marrow signal intensity compared to muscle (midfemoral marrow/muscle ratio range 1.35–1.69). Both normal dogs had midfemoral marrow to muscle ratios of 1.6–1.69. However, there were 3 lymphoma-affected dogs and one of the MDS-affected dogs that had marrow to muscle ratios in a numerical range (0.65–1.1), which was less than or nearly equal to the MDS dogs. Therefore, 2 of the MDS and 1 of the lymphoma-affected dogs were within 10% of being isointense to regional skeletal muscle (point ROI midfemoral marrow/muscle ratio of 1.0), 2 lymphoma dogs and one of the MDS dogs had

midfemoral marrow/muscle ratios less than 0.75, and the 2 normal dogs and 4 of the lymphoma dogs were greater than 1.35. The clinically normal dogs and the 7 lymphoma-affected dogs were not as distinguishable from each other based on bone marrow appearance on the other 4 sequences used here (Table 1).

The bone marrow cellularity for the 7 lymphoma-affected dogs was either within or below reference intervals. By comparison, the MDS dogs had greater cellularity as well as % blast cells at least twice that of any of the lymphoma-affected dogs. Based on the out-of-phase sequence, the hypercellular marrow induced by the MDS condition, tended to resemble skeletal muscle in signal intensity for lumbar vertebral and midfemoral regions both visually and generally numerically rather than be notably different from it as was found in either the lymphoma-affected or the normal dogs.

Discussion

Despite the absence of focal or multifocal bone marrow lesions among the 10 affected dogs, the visual assessment of marrow signal intensity on the Out-of-Phase pulse sequence generally distinguished the 3 dogs with MDS from the other dogs with or without lymphoma of the marrow and from the normal dogs. Basically, vertebral and midfemoral marrow regions of the MDS-affected dogs had signal intensities visibly similar to that of regional skeletal muscle and visibly different from fat or urinary bladder on the Out-of-Phase sequence. On that sequence @ 3T, the normal vertebral marrow signal intensities are visibly less than those from regional skeletal muscle. We assumed that normal adult dog vertebral marrow signal is low due from suppression induced in the Out-of-Phase sequence because of the approximately equal red (cellular) and yellow (fatty) marrow and the influence of regional trabecular bone and other factors.[7,12] Similarly, the normal middiaphyseal femoral marrow signal intensities are visibly greater than those from the regional skeletal muscle on the Out-of-Phase sequence @ 3T. We suspect that the normal femoral middiaphyseal adult dog marrow signal is high because of the presumed predominance of yellow marrow with limited signal suppression on the Out-of-Phase sequence.[7,12] The skeletal muscle, although subject to atrophy, edema, fat infiltrate and other conditions, still serves as a reasonably predictable basis for comparison to the marrow. MR sequence parameters as well as numerous physiologic and pathologic processes influence the MR appearance of both normal and abnormal bone marrow.[41] These observations suggest that the visual comparison of marrow signal intensity to an internal standard like regional skeletal muscle has merit in the recognition of diffuse, hypercellular infiltrative marrow disease on whole body images. The point region of interest numeric analyses had more complicated interpretations. However, the normal dogs and the majority of the lymphoma-affected dogs had midfemoral marrow of greater signal intensity than regional muscle and all of the normal and lymphoma-affected dogs had lumbar vertebral marrow of less signal intensity than regional muscle. However, much more research into both the physical and physiologic influences will be necessary to further explain the potential variables that are beyond the scope of this study.

The comparison of the "visual" relative signal intensity between marrow and muscle at the 2 sites evaluated here has merit in that a vertebral or midfemoral signal intensity similar to regional skeletal muscle should arouse suspicion of marrow abnormality. Hypercellular marrow seems to be a contributing factor. There are some inconsistencies when point ROI-based analyses were applied to the midfemoral marrow. Here, there was overlap between the MDS-affected dogs and the lymphoma-affected dogs, but not the normal dogs. There was 1 lymphoma-affected, but marrow negative dog that had measured bone marrow signal intensity close to skeletal muscle. One of the MDS dogs and 2 of the lymphoma-affected dogs had measured midfemoral marrow signal intensity less than that of skeletal muscle. Because of the small dog numbers, we chose not to speculate further as to potential marrow or MRI technical variables that may be involved here. At this point, point ROI-based similarity of midfemoral signal intensity to that of regional skeletal muscle still distinguished 2 of the 3 MDS dogs from both of the normal dogs and all but one of the lymphoma-affected dogs. Our data suggest that normal dogs and most dogs without hypercellular marrow will have ROI-based midfemoral marrow signal intensity different (greater than or less than) from that of regional skeletal muscle. Comparison between the signal intensity characteristics of the middiaphyseal femoral and the midlumbar vertebral body marrow signal intensity seems to provide additional perspective for ROI interpretation.

There are a number of considerations surrounding our results. First, it is possible that the small number of dogs we studied simply lacked focal or sufficiently severe diffuse lymphoma marrow infiltrate for us to identify it with MR or confirm with standard sampling techniques. Second, it is possible that lymphoma marrow infiltrate in dogs can be diffuse, focal or multifocal making marrow involvement difficult to differentiate from normal variation as was seen in the one dog (of 7) with B-cell lymphoma. Third, it is also possible that the pulse sequences we used were unable to detect the lymphoma-related marrow disease present. More likely, however, is that this is a function of the severity of marrow infiltration. The one B-cell affected dog with demonstrable marrow involvement did not have hypercellular marrow. Our results suggest that it is the hypercellularity of the marrow that at least in part creates the visual similarity between marrow and muscle on the Out-of-Phase sequence in the MDS-affected dogs in both the midfemur and lumbar vertebral regions. It is assumed that with hypercellular marrow, the signal contributions from the fat and the marrow elements in the midlumbar vertebral and midfemoral

regions are similar to the contributions from the mixture of regional fat and muscle elements on the Out-of-Phase sequence used here. By comparison, at 3T, the relative contributions of fat and marrow elements are apparently more equal in the vertebral marrow resulting in the low signal intensity (as well as the effect of marrow trabeculae) and more dominated by fat in the midfemoral marrow resulting in the high marrow signal intensity in the midfemoral marrow in the dogs with normal marrow cellularity. That raises the question as to whether sufficiently hypercellular lymphoma marrow infiltrates would be detectable and whether it would be isointense to regional skeletal muscle? It also raises the question about the MR appearance of "stimulated" normal marrow as is seen in dogs with conditions such a hemolytic anemia and whether that would become isointense to regional skeletal muscle?

Acknowledging that bone marrow infiltrate in canine lymphoma occurs with sufficient frequency to affect prognosis,[6,42] the question now is whether additional data on a different subset of lymphoma-affected dogs with high marrow cellularity will resemble the MDS-affected dogs'appearance here? We used mature, but not aged normal dogs used as controls in this pilot study for comparison to aged dogs with chronic disease. Acknowledging that younger dogs are generally more likely to have highly cellular marrow than older dogs,[43] this should theoretically reduce the ability to detect differences in marrow signal intensity between dogs with normal marrow and those with as we hypothesize hypercellular marrow. Because the differences were visible here, there is less concern for the age difference. In a more comprehensive study, age-matched control dogs and greater dog numbers would be appropriate.

A similar study of abdominal parenchymal organ signal intensity was also conducted on this group of dogs and reported elsewhere.[44] Relative signal intensity again using skeletal muscle on the T2W sequence as a basis for abdominal parenchymal organ comparison distinguished the normal from the affected dogs acknowledging that the signal intensity variation may be because of the malignancy or it may be because of metabolic abnormalities induced by the cancer condition. The 2 clinically normal dogs were a feasibility assessment for using MR signal intensity as part of the interpretive background for high-field whole body imaging of diffuse infiltrative abnormalities (disease that does not alter the tissue or organ architecture) including the bone marrow. Despite the qualitative nature of grouping signal intensity values using only visual comparisons on the Out-of-Phase sequence and without specific focus on marrow regions, the 2 clinically normal dogs' signal intensities for the lumbar vertebral or midfemoral marrow regions and the skeletal muscle regions provided a useful perspective for evaluation of the abnormal dogs. It should be emphasized that the femoral marrow signal intensity comparisons are only valid for the midshaft region because of the marrow differences known to occur in the metaphyses and epiphyses in adult dogs.[7] The out-of-phase pulse sequence was not reported in earlier low-field investigations.[7,8] We also raise concern for field strength variations in marrow observations in adult dogs because the lumbar marrow has a visibly greater signal intensity than skeletal muscle on a T1W sequence @ 3T while it is reported to be of equal signal intensity to skeletal muscle on low-field equipment.[7] Additionally, the long bone marrow has basically the same visible signal intensity as skeletal muscle on STIR sequences @ 3T while it is reported to be less signal intense than skeletal muscle on low-field equipment.[7] Therefore, there are not only differences related to the parameters used in the various pulse sequences and machine to machine variations, but there also seems to be a difference between high- and low-field techniques. These differences will likely affect interpretation of diffuse marrow and potentially parenchymal organ disease. Further study is obviously indicated at both field strengths.

Footnotes

[a] 3T HDX, General Electric Medical Systems, Milwaukee, WI
[b] Carestream Health, Inc, Rochester, NY

Acknowledgment

Funding provided by the Academic Health Center Seed Grant Program.

Conflict of Interest: Authors disclose no conflict of interest.

References

1. Johnson C, Brennan S, Ford S, Eistace S. Whole-body MR imaging: Applications in oncology. Europ J Cancer Surg 2006;32:239–246.

2. Barth MM, Smith MP, Pedrosa I, et al. Body MR imaging at 3.0 T: Understanding the opportunities and challenges. Radiographics 2007;27:1445–1462.

3. Ladd SC, Ladd ME. Perspectives for preventive screening with total body MRI. Eur Radiol 2007;17:2889–2897.

4. Schmidt GP, Reiser MF, Baur-Melnyk A. Whole-body MRI for the staging and follow-up of patients with metastasis. Eur J Radiol 2009;70:393–400.

5. Kraft S, Randall E, Wilhelm M, Lana S. Development of a whole-body magnetic resonance imaging protocol for normal dogs and canine cancer patients. Vet Radiol Ultrasound 2007;48:212–220.

6. Raskin RF, Krehbiel JD. Prevalence of leukemic, blood and bone marrow in dogs with multicentric lymphoma. J Am Vet Med Assoc 1989;194:1427–1429.

7. Armbrust LJ, Hoslinson JJ, Biller DS, Wilkerson M. Low-field magnetic resonance imaging of bone marrow in the lumbar spine, pelvis and femur in the adult dog. Vet Radiol Ultrasound 2004;45:393–401.

8. Armbrust LJ, Ostmeyer M, McMurphy R. Magnetic resonance imaging of bone marrow in the pelvis and femur of young dogs. Vet Radiol Ultrasound 2008;49:432–437.

9. Alyas F, Saifuddin A, Connell D. MR imaging evaluation of the bone marrow and marrow infiltrative disorders of the lumbar spine. Magn Reson Imaging Clin N Am 2007;15:199–219.

10. Carroll KW, Feller JF, Tirman PFJ. Useful internal standards for disgintuishing infiltrative marrow pathology from hematopoetic marrow at MRI. J Magn Reson Imaging 1997;7: 394–398.

11. Murphy DT, Moynagh MR, Eustace SJ, Kavanagh EC. Bone marrow. Magn Reson Imaging Clin N Am 2010;18: 727–735.

12. Shah LM, Hanrahan CJ. MRI of spinal bone marrow: Part 1, techniques and normal age-related appearances. Am J Roentgenol 2011;197:1298–1308.

13. Swartz PG, Roberts CC. Radiological reasoning: Bone marrow changes on MRI. Am J Roentgenol 2009;193:S1–S4.

14. Zajick DC, Morrison WB, Schweitzer ME, et al. Benign and malignant processes: Normal values and differentiation with chemical shift MR imaging in vertebral marrow. Radiology 2005;237:590–596.

15. Jemal A, Tiwari RC, Murray T, et al. Cancer statistics, 2004. CA Cancer J Clin 2004;54:8–29.

16. Danrad R, Martin DR. MR imaging of diffuse liver diseases. Magn Reson Imaging Clin N Am 2005;13:277–293.

17. Ollivier L, Gerber S, Vanel D, et al. Improving the interpretation of bone marrow imaging in cancer patients. Cancer Imaging 2006;6:194–198.

18. Vail DM, Young KM. Canine lymphoma and lymphoid leukemia. In Withrow and MacEwen's Small Animal Clinical Oncology, 4th ed. Philadelphia, PA: Elsevier/Saunders; 2007; 699–733.

19. Alustiza JM, Castiella A, De Juan MD, et al. Iron overload in the liver diagnostic and quantification. Eur J Radiol 2007;61:499–506.

20. Kuhn JP, Hegenscheid K, Siegmund W, et al. Normal dynamic MRI enhancement patterns of the upper abdominal organs: Gadoxetic acid compared with gadobutrol. Am J Roentgenol 2009;193:1318–1323.

21. Schneider G, Uder M. Contrast-enhanced magnetic resonance body imaging 5. Top Magn Reson Imaging 2003;14:403–425.

22. Shao-Pow L, Brown JJ. MR contrast agents: Physical and pharmacologic basics. J Magn Reson Imaging 2007;25:884–899.

23. Lee VS, Hecht EM, Taouli B, et al. Body and cardiovascular imaging at 3.0T. Radiology 2007;244:692–705.

24. Li T, Mirowitz SA. T2-weighted echo planar MR imaging of the abdomen: Optimization of imaging parameters. Clin Imaging 2003;27:124–128.

25. Martin DR, Friel HT, Danrad R, et al. Approach to abdominal imaging at 1.5 tesla and optimization at 3 tesla. Magn Reson Imaging Clin N Am 2005;13:241–254.

26. Applegate KE, Maglinte DD. Imaging of the bowel in children: New imaging techniques. Pediatr Radiol 2008;38:S272–S274.

27. Cronin CG, Lohan DG, Browne AM, et al. Magnetic resonance enterography in the evaluation of the small bowel. Semin Roentgenol 2009;44:237–243.

28. Fenchel M, Kramer U, Nael K, Miller S. Cardiac magnetic resonance imaging at 3.0 T. Top Magn Reson Imaging 2007;18:95–104.

29. Kuo R, Panchal M, Tanenbaum L, Crues JV. 3.0 Tesla imaging of the musculoskeletal system. J Magn Reson Imaging 2007;25:245–261.

30. Robinson PJ. The effects of cancer chemotherapy on liver imaging. Eur Radiol 2009;19:1752–1762.

31. Taouli B, Ehman RL, Reeder SB. Advanced MRI methods for assessment of chronic liver disease. Am J Roentgenol 2009;193:14–27.

32. Copen WA, Schwamm LH, Gonzalez RG, et al. Ischemic stroke: Effects of etiology and patient age on time course of the core apparent diffusion coefficient. Radiology 2001;221:27–34.

33. Zha Y, Li M, Yang J. Dynamic contrast enhanced magnetic resonance imaging of diffuse spinel bone marrow infiltration in patients with hematological malignancies. Korean J Radiol 2010;11:187–194.

34. Akisik FM, Sandrasegaran K, Aisen AM, et al. Abdominal MR imaging at 3.0 T. Radiographics 2007;27:1433–1444.

35. Bydder GM, Chung CB. Magnetic resonance imaging of short T2 relaxation components in the musculoskeletal system. Skeletal Radiol 2009;38:201–205.

36. Colagrande S, Centi N, Galdiero R, Ragozzino A. Transient hepatic intensity differences: Part 2, those not associated with focal lesions. Am J Roentgenol 2007;188:160–166.

37. de Bazelaire CM, Duhamel GD, Rofsky NM, Alsop DC. MR imaging relaxation times of abdominal and pelvic tissues measured in vivo at 3.0 T: Preliminary results. Radiology 2004;230:652–659.

38. Valli VE, San Myint M, Barthel A, et al. Classification of canine malignant lymphomas according to the World Health Organization criteria. Vet Pathol 2011;48:198–211.

39. Tefferi A, Vardiman JW. Myelodysplatic syndromes. New Eng J Med 2009;361:1872–1885.

40. Weiss DJ. A retrospective study of the incidence and the classification of bone marrow disorders in the dog at a veterinary teaching hospital (1996-2004). J Vet Int Med 2006;20:955–961.

41. Seiderer M, Staebler A, Wagner H. MRI of bone marrow: Opposed-phase gradient echo sequences with long repetition time. Eur Radiol 1999;9:652–661.

42. Modiano JF, Breen M, Valli VE, et al. Predictive value of p16 or Rb inactivation in a model of naturally occurring canine non-Hodgkin's lymphoma. Leukemia 2007;21:184–187 (letter).

43. Moritz A, Bauer NB, Weiss DJ, et al. Evaluation of bone marrow. In: Weiss DJ, Wardrop KJ, eds. Schalm's Veterinary Hematology, 6th ed. Ames, IA: Wiley Blackwell; 2010:1039–1046.

44. Feeney DA, Sharkey LC, Steward SM, et al. Parenchymal organ signal intensity in 3T body MRI of canine hematopoetic neoplasia: A pilot animal model study. Comp Med 2013;63:1–9.